J Biomol NMR (2007) 37:303–312
DOI 10.1007/s10858-007-9143-0

ARTICLE

Combined solid state and solution NMR studies of α,ε-^{15}N labeled bovine rhodopsin

Karla Werner · Ines Lehner · Harpreet Kaur Dhiman · Christian Richter · Clemens Glaubitz · Harald Schwalbe · Judith Klein-Seetharaman · H. Gobind Khorana

Received: 5 January 2007 / Accepted: 8 January 2007 / Published online: 23 February 2007

Abstract Rhodopsin is the visual pigment of the vertebrate rod photoreceptor cell and is the only member of the G protein coupled receptor family for which a crystal structure is available. Towards the study of dynamics in rhodopsin, we report NMR-spectroscopic investigations of α,ε-^{15}N-tryptophan labeled rhodopsin in detergent micelles and reconstituted in phospholipids. Using a combination of solid state ^{13}C,^{15}N-REDOR and HETCOR experiments of all possible $^{13}C'_{i-1}$ carbonyl/$^{15}N_i$-tryptophan isotope labeled amide pairs, and H/D exchange ^{1}H,^{15}N-HSQC experiments conducted in solution, we assigned chemical shifts to all five rhodopsin tryptophan backbone ^{15}N nuclei and partially to their bound protons. ^{1}H,^{15}N chemical shift assignment was achieved for indole side chains of Trp35$^{1.30}$ and Trp175$^{4.65}$. ^{15}N chemical shifts were found to be similar when comparing those obtained in the native like reconstituted lipid environment and those obtained in detergent micelles for all tryptophans except Trp175$^{4.65}$ at the membrane interface. The results suggest that the integrated solution and solid state NMR approach presented provides highly complementary information in the study of structure and dynamics of large membrane proteins like rhodopsin.

Keywords GPCR · HSQC · Membrane proteins · REDOR · Rhodopsin · Tryptophan

Abbreviations

NMR	nuclear magnetic resonance
HSQC	heteronuclear single quantum correlation
TROSY	transverse relaxation optimized spectroscopy
SS-MAS	solid state magic angle spinning
REDOR	rotational echo double resonance
HEK293S	suspension growth adapted human embryonic kidney cell line
DM	dodecyl maltoside
OG	octyl glucoside

K. Werner · I. Lehner · C. Richter · C. Glaubitz · H. Schwalbe (✉) · J. Klein-Seetharaman
Center for Biomolecular Magnetic Resonance, Johann Wolfgang Goethe-Universität Frankfurt, Max-von-Laue-Str. 7, 60438 Frankfurt/Main, Germany
e-mail: schwalbe@nmr.uni-frankfurt.de

K. Werner · C. Richter · H. Schwalbe · J. Klein-Seetharaman
Institute of Organic Chemistry and Chemical Biology, Johann Wolfgang Goethe-Universität Frankfurt, Max-von-Laue-Str. 7, 60438 Frankfurt/Main, Germany

I. Lehner · C. Glaubitz
Institute of Biophysical Chemistry, Johann Wolfgang Goethe-Universität Frankfurt, Max-von-Laue-Str. 9, 60438 Frankfurt/Main, Germany

H. K. Dhiman · J. Klein-Seetharaman
Department of Structural Biology, University of Pittsburgh School of Medicine, 3501 Fifth Avenue, Pittsburgh, PA 15261, USA

H. G. Khorana (✉)
Departments of Biology and Chemistry, Massachusetts Institute of Technology, 77 Massachusetts Avenue, Cambridge, MA 02139, USA
e-mail: khorana@mit.edu

DOPC 1,2-dioleoyl-*sn*-glycero-3-phosphocholine
GPCR G-protein coupled receptors
amino acids are designated by the three-letter abbreviation

Introduction

G protein coupled receptors (GPCRs) form the largest family of signaling proteins within the human genome. The only known structure of any GPCR is that of visual photoreceptor rhodopsin in its inactive state (Palczewski et al. 2000). In this state, rhodopsin's covalently bound retinal chromophore is in the 11-*cis* conformation. Illumination causes isomerization to *all-trans* retinal which triggers changes in the structure of the protein that result in an active conformation, Metarhodopsin II. Biophysical studies indicate that light-activation is accompanied by helix movements leading to an opening of the helical bundle at the cytoplasmic side (Hubbell et al. 2003). A crystal structure of light-exposed rhodopsin has been published recently, but its low resolution still precludes understanding the structural details (Salom et al. 2006). Recent modeling results indicate that motions accessible to the dark structure are compatible with the changes observed upon light-activation (Isin et al. 2006). Our long-term goal is to describe dynamics and conformational changes in the rhodopsin structure accurately with NMR spectroscopic methods.

Applicability of both solution and solid state NMR spectroscopy to the study of rhodopsin has already been demonstrated. In solution, ^{19}F labels introduced in the cytoplasmic face of rhodopsin showed distinct chemical shifts and changes upon illumination (Klein-Seetharaman et al. 1999) and nuclear Overhauser effects were observed between defined pairs of ^{19}F labels (Loewen et al. 2001). A study on α-^{15}N-lysine labeled rhodopsin revealed high flexibility of the cytoplasmic C-terminus (Klein-Seetharaman et al. 2002), which was also confirmed by NMR studies of rhodopsin ^{31}P-labeled at its phosphorylation sites in the C-terminus (Getmanova et al. 2004). Finally, solution NMR of α,ε-^{15}N-tryptophan labeled rhodopsin revealed the general feasibility to observe the signals of residues within the central core of the membrane protein (Klein-Seetharaman et al. 2004). Solid state NMR originally addressed questions related to retinal ligand structure including high precision bond length and angle determinations (Feng et al. 2000; Carravetta et al. 2004; Spooner et al. 2004). More recently, ligand-protein contacts and changes upon illumination have been identified (Verdegem et al. 1999; Patel et al. 2004; Patel et al. 2005; Crocker et al. 2006).

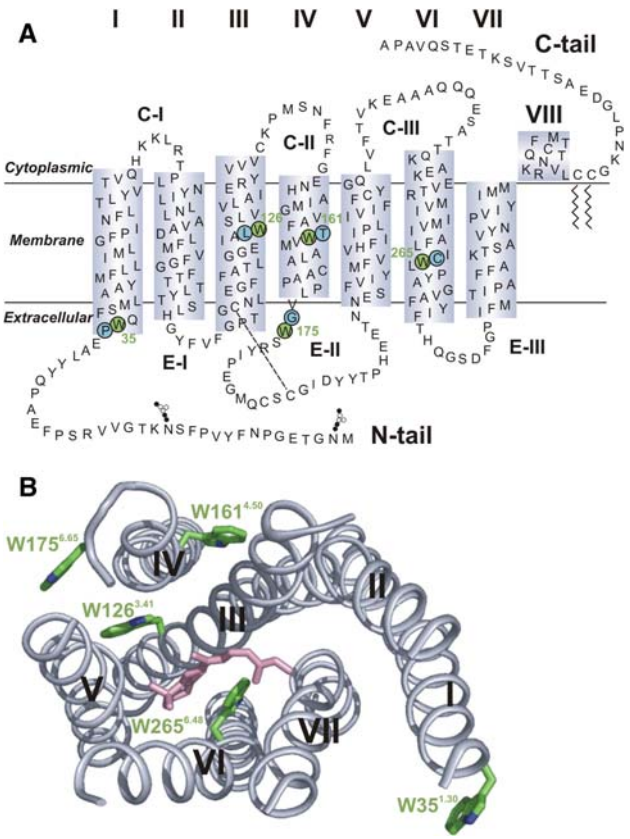

Fig. 1 (**a**) Secondary structure model of bovine rhodopsin with the five tryptophans indicated in green and the *i*–1 amino acids highlighted in blue. (**b**) The three-dimensional structure model of the transmembrane domains of bovine rhodopsin based on the crystal structure shows the orientation of the five tryptophans. 11-*cis*-retinal is highlighted in pink

These NMR studies support earlier conclusions that tryptophan residues play an important role in the activation process. There are five tryptophan residues in rhodopsin: Trp35$^{1.30}$, Trp126$^{3.41}$, Trp161$^{4.50}$, Trp175$^{4.65}$ and Trp265$^{6.48}$ (Fig. 1a). The superscript in residue numbers refers to the general Ballesteros and Weinstein GPCR numbering scheme (Ballesteros and Weinstein 1995). Trp35$^{1.30}$ and Trp175$^{4.65}$ are situated at the extracellular end of the transmembrane helices (Fig. 1b) and are not very highly conserved in the GPCR family. In contrast, tryptophans at positions 126$^{3.41}$, 161$^{4.50}$ and 265$^{6.48}$ are located within the transmembrane domain (Fig. 1b) and are highly conserved (Patel et al. 2005). Early linear dichroism (Chabre and Breton 1979) and UV absorbance (Rafferty et al. 1980) measurements showed that the conformation of at least one tryptophan is affected by light activation, and further site-directed mutagenesis

attributed the observed changes to Trp126$^{3.41}$, Trp161$^{4.50}$ and Trp265$^{6.48}$(Lin and Sakmar 1996). Trp126$^{3.41}$ and Trp265$^{6.48}$ are part of the retinal binding pocket (Nakayama and Khorana 1990; Nakayama and Khorana 1991; Palczewski et al. 2000; Li et al. 2004). The side chain of Trp265$^{6.48}$ in particular is in close contact with the ionone ring and is thus well suited to couple isomerization of the chromophore with helix motion. The solid state NMR experiments performed with ^{15}N- and ^{13}C-tryptophan labeled rhodopsin (Patel et al. 2005; Crocker et al. 2006) revealed a weakening of hydrogen bonds between the indole nitrogens of Trp126$^{3.41}$ and Trp265$^{6.48}$ and other amino acids upon illumination (Patel et al. 2005). Furthermore, contacts between Trp265$^{6.48}$ and the C20-methyl group of the retinal are lost (Crocker et al. 2006) and a new contact is formed with the C19-methyl group.

In the previous NMR studies, only Trp265$^{6.48}$ was assigned using solid state NMR and site directed mutagenesis (Patel et al. 2005). Since Trp265$^{6.48}$ is a conserved residue and its mutation affects ligand binding and activity of rhodopsin (Reeves et al. 1999), a less invasive assignment method would be advantageous. We report here the non-invasive assignment of the backbone resonances of all five tryptophan residues using a combination of solution and solid state NMR spectroscopy of ^{13}C- and ^{15}N-isotope labeled rhodopsin.

Materials and methods

Expression and purification of selectively isotope labeled rhodopsin in HEK293S cell lines

Rhodopsin was expressed in a tetracycline-inducible HEK293S cell line stably transfected with the wild-type opsin gene (Reeves et al. 2002). Cells were grown in spinner flasks in media prepared from individual components (Sigma) as described (Reeves et al. 1996). Cells were harvested on day 6 and resuspended in 25 ml/liter cell culture of buffer A (137 mM NaCl, 2.7 mM KCl, 1.8 mM KH_2PO_4, 10 mM Na_2HPO_4, pH 7.2). 11-*cis* retinal prepared from *all-trans* retinal (Sigma) (Knowles and Priestley 1978) was added at a final concentration of 40 μM. The protein was solubilized with 1% DM and purified by immunoaffinity chromatography. The 1D4 antibody (University of British Columbia, Vancouver, Canada) was coupled to activated Sepharose 4B (Sigma) as described (Oprian et al. 1987). Rhodopsin was bound to the beads and washed with 20 columns of buffer B (buffer A + 0.05% DM).

Preparation of solid state NMR samples

Samples for solid state NMR measurements were further washed with 10 column volumes of buffer C (2 mM NaH_2PO_4/Na_2HPO_4 + 0.05 DM, pH 6.0) followed by 20 column volumes of buffer D (2 mM NaH_2PO_4/Na_2HPO_4 + 1.46 OG, pH 6.0). Rhodopsin was eluted in buffer D containing 150 μM of the nonapeptide corresponding to the 1D4 epitope. Reconstitution in DOPC (Avanti Polar Lipids, Alabaster, AL) used a procedure described in (Eilers et al. 2002). The pelleted proteoliposomes containing 5–6 mg of protein were transferred into NMR rotors and snap frozen in liquid nitrogen and stored at –80°C until the measurements.

Preparation of liquid state NMR samples

For solution state NMR experiments, rhodopsin bound to 1D4-beads was washed with 20 columns of buffer E (2 mM NaH_2PO_4/Na_2HPO_4 + 0.05% d_{25}-DM, pH 6.0). The protein was eluted as described for solid state NMR samples in buffer E containing 150 μM nonapeptide. Buffer exchange and concentration was performed as described (Klein-Seetharaman et al. 1999) yielding 5–6 mg protein in 220 μl of Buffer F (20 mM NaH_2PO_4/Na_2HPO_4, 10% D_2O, pH 6.5).

NMR spectroscopy

Liquid NMR experiments were carried out on a Bruker 900 MHz spectrometer, equipped with a 5 mm HCN cryogenic probe and z-axis gradient at a temperature of 310 K. Spectra were recorded in 90% H_2O/10% D_2O using a WATERGATE (Piotto et al. 1992) pulse sequence for water suppression. ^{1}H chemical shifts were referenced directly to 3-(trimethylsilyl)-1-propane-sulfonic acid sodium salt (Sigma) at 0.0 ppm, whereas ^{15}N was indirectly referenced. Modified ^{1}H,^{15}N-HSQC spectra with and without ^{13}C/^{15}N decoupling where recorded in an interleaved manner as a single data set. Standard ^{1}H,^{15}N-HSQC spectra were performed on samples dissolved in D_2O. Data were collected with 2K data points and 512-1K scans average per FID.

Solid state experiments were run on a Bruker 600 MHz spectrometer using 4-mm MAS probes. Samples were maintained at 220 K for the duration of the measurements at a sample spinning rate of 8 kHz. ^{1}H and ^{13}C chemical shifts were externally referenced to tetramethylsilane (Sigma) at 0.0 ppm and ^{15}N chemical shifts to $(NH_4)_2SO_4$ at 27.0 ppm. Proton decoupling during acquisition was achieved using two

pulse phase modulation and a proton decoupling field strength of 64 kHz. CPMAS experiments (Metz et al. 1994) utilized 60–80% ramped contact times of 500 μs for the ^{15}N nuclei. Usually 4K or 6K scans were recorded.

^{15}N-detected ^{13}C/^{15}N REDOR (Gullion and Schaefer 1989) experiments used 60–80% ramped cross polarization with a contact time of 500 μs. Two equally spaced dephasing ^{13}C 180°-pulses were applied per rotor period and one refocusing ^{15}N 180°-pulse was applied in the center of the rotor period. Optimal dephasing was observed at 62 rotor cycles (7.75 ms) and used for all experiments. Typically 25K scans or 50K scans were recorded.

^{15}N/^{1}H two dimensional heteronuclear spectroscopy (HETCOR) (van Rossum et al. 1997) was performed using frequency switched Lee-Goldburg decoupling at an effective proton decoupling field of 85 kHz during the evolution period and two pulse phase modulation proton decoupling at 64 KHz during the acquisition period. 2K scans in the ω_2 dimension and 64 rows in the ω_1 dimension were acquired using time-proportional phase increments. The scaling factor for the ω_1 dimension was determined to be 0.575.

All data were acquired using Bruker software xwinnmr version 3.5. Spectra were processed and analyzed with Topspin version 1.3 (Bruker).

Results

Isotope labeling scheme

The following isotope labeling scheme for assignment of ^{15}N-tryptophan labeled rhodopsin was applied similar to previous studies of rhodopsin (Klein-Seetharaman et al. 2002) and bacteriorhodopsin (Mason et al. 2005): in addition to introduction of α,ε-^{15}N-labeled tryptophan we introduced specific backbone carbonyl ^{13}C labels in the *i*–1th position using amino acids enriched with ^{13}C at least at the C′ position. Each of the five tryptophan residues in rhodopsin is preceded by a unique type of amino acid in the primary structure of rhodopsin (Fig. 1). These are proline, leucine, glycine, threonine and cysteine for Trp35$^{1.30}$, Trp126$^{3.41}$, Trp161$^{4.50}$, Trp175$^{4.65}$ and Trp265$^{6.48}$, respectively. For both solution and solid state NMR experiments, we thus prepared rhodopsin samples with unique $^{13}C'_{i-1}/^{15}N_i$ pairs and utilized NMR spectroscopic strategies to identify tryptophan resonances based on their coupling to the *i*–1 amino acid.

Solid state NMR tryptophan resonance assignment

In solid state NMR experiments of rhodopsin reconstituted in DOPC lipids, dipolar couplings between the adjoining NMR active atoms were measured using the rotational echo double resonance experiment (REDOR). Assignment of signals is based on the fact that introduction of dephasing pulses causes significant reduction in the intensity of single resonances, as the directly bound nucleus of the ^{13}C/^{15}N pair in the samples are only 1.3 Å apart (Mason et al. 2005).

^{15}N detected cross polarization (CP) experiments carried out at 310 K yielded spectra with poor signal-to-noise ratios indicating slow protein tumbling at the μs timescale, which interferes with refocusing and decoupling of the MAS signal. In contrast, rapid freezing of the samples in liquid nitrogen and measurements recorded at 220 K gave well-resolved spectra with a good signal-to-noise ratio. Rapid freezing was found critical for a good spectra quality. Starting measurements at low temperatures, going stepwise to higher temperatures and return to low temperatures resulted in broad, poorly resolved lines. It is likely that slow freezing and thawing of the samples causes heterogeneities in structure and dynamics of rhodopsin.

The ^{15}N CP spectrum of α,ε-^{15}N-tryptophan labeled rhodopsin in DOPC is shown in Fig. 2a. It displays features very similar to the spectra of rhodopsin in DM detergent reported by Patel et al. (2005). The poorly resolved resonances between 129 ppm and 140 ppm correspond to the indole side-chain resonances and the three resolved resonances between 110 ppm and 126 ppm to backbone signals. Additionally, a signal at 125.7 ppm was observed with variable intensity in different samples.

Assignment of the three resolved backbone resonances using the REDOR technique is shown in Fig. 2b–d. The resonance at 117.3 ppm was thus assigned to the backbone amide of Trp126$^{3.41}$and the resonance at 122.3 ppm to Trp161$^{4.50}$. For the sample prepared to assign Trp265$^{6.48}$, a strong dephasing was observed at 111.5 ppm, confirming the previous result of Patel et al (Patel et al. 2005). A small effect was detected for the Trp35$^{1.30}$ sample (Fig. 2e) at 125.7 ppm but was very close to the noise level. For Trp175$^{4.65}$, some changes in the entire backbone area and a clear loss of intensity particularly at 111.5 ppm (Fig. 2f) was observed. This resonance is overlapping with the resonance of Trp265$^{6.48}$. In an attempt to achieve better resolution, the CP spectrum was expanded in a 2D ^{15}N,^{1}H HETCOR experiment, shown

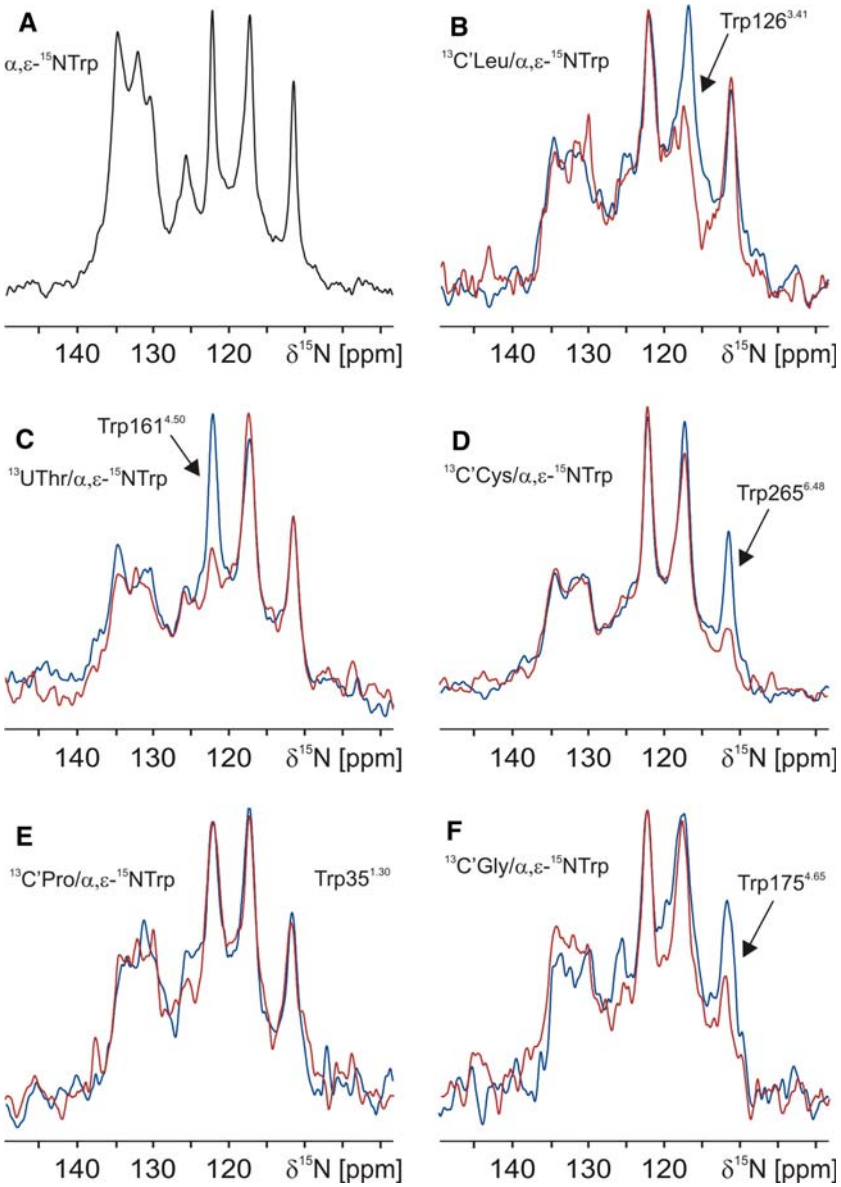

Fig. 2 Dephased (red line) and non-dephased (blue line) ^{15}N detected $^{13}C/^{15}N$ CP REDOR spectra of selectively labeled rhodopsin in DOPC lipid bilayers at 220 K. (**a**) α,ε-^{15}N-Trp. (**b**) $^{13}C'$-Leu/α,ε-^{15}N-Trp. (**c**) ^{13}U-Thr/α,ε-^{15}N-Trp. (**d**) $^{13}C'$-Cys/α,ε-^{15}N-Trp. (**e**) $^{13}C'$-Pro/α,ε-^{15}N-Trp. (**f**) $^{13}C'$-Gly/α,ε-^{15}N-Trp

in Fig. 3. This resulted in unambiguous identification of the 125.7 ppm signal as a backbone resonance. However, resolution enhancement was not sufficient to further resolve the side-chain signals or to separate the Trp175$^{4.65}$ and Trp265$^{6.48}$ resonances.

Liquid state NMR results

Figure 4 shows $^{1}H,^{15}N$-HSQC spectra of α,ε-^{15}N Trp labeled bovine rhodopsin solubilized in partially deuterated DM in solution. Five resonances in the indole region and five signals for the protein backbone are observed. Several weak additional peaks in the backbone region were also detected. We attribute them to natural abundance signals originating from very flexible regions probably in the C-terminus (K. Werner et al., unpublished results). Two of the backbone signals at 7.7 ppm and 8.3 ppm are more intense as compared to the remaining three resonances and therefore likely arise from the more flexible interface tryptophans Trp175$^{4.65}$ and Trp35$^{1.30}$. Similarly, two of the indole resonances at 10.6 ppm and 11.4 ppm show a higher intensity compared to the other side chain signals. A 4-h standard $^{1}H,^{15}N$-HSQC spectrum of a

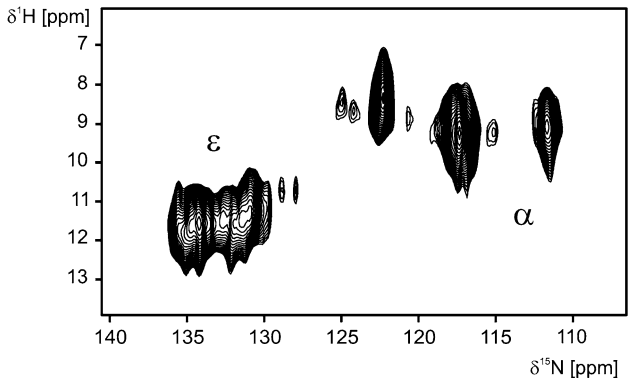

Fig. 3 ^{15}N detected ^{15}N,^{1}H HETCOR experiment of α,ε-^{15}N-Trp at 220 K in lipid bilayers, backbone and indole signals are labeled with "α" and "ε" respectively

α,ε-^{15}N Trp sample recorded 2 h after dissolving the sample in D_2O at 4°C showed the loss of the backbone peak at 8.3 ppm and the indole resonance at 10.6 ppm (indicated by arrows in Fig. 4). Although both Trp175$^{4.65}$ and Trp35$^{1.30}$ are expected to be solvent exposed based on the crystal structure (Palczewski et al. 2000), Trp175$^{4.65}$ is the only tryptophan that is not part of a transmembrane helix (Fig. 1b). We therefore conclude that the 8.3/10.6 ppm pair arises from Trp175$^{4.65}$. This implies that the 7.7/11.4 ppm pair arises from Trp35$^{1.30}$.

Rhodopsin solubilized in detergent micelles represents a system with an effective size of approx. 150 kD (Jastrzebska et al. 2004), making it challenging for liquid NMR spectroscopy due to signal overlap and rapid relaxation. Initially, standard heteronuclear experiments such as a proton detected HNCO as well as a carbon detected CN experiments

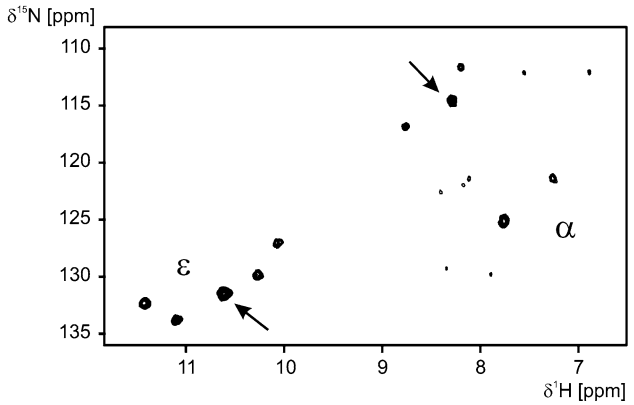

Fig. 4 ^{1}H, ^{15}N HSQC solution NMR spectra of 0.5 mM [α, ε]-^{15}N-Trp rhodopsin in d_{25}-DM at 310 K, backbone and indole signals are labeled with "α" and "ε" respectively. The signals which disappear upon solvent exchange are indicated with arrows

were applied in order to obtain the desired sequential correlation. As in previous HNCO experiments designed to assign lysine backbone resonances in α-^{15}N-lysine labeled rhodopsin, no cross peaks were obtained. This is in contrast to the lysine residue located in the flexible C-terminus, where an HNCO cross peak was obtained for Lys339 (Klein-Seetharaman et al. 2002).

Next, 2D ^{1}H,^{15}N-HSQC spectra were compared with and without ^{13}C/^{15}N scalar coupling. Routinely, ^{13}C/^{15}N decoupling is implemented in ^{1}H,^{15}N correlation spectra in order to avoid loss of magnetization during the transfer pathway. We took advantage of this coupling effect running pairs of two-dimensional spectra for each sample in an interleaved manner to correct for the long-term instrumental drift. Thus in the course of the experiment every individual FID was collected with and without suppressing ^{13}C/^{15}N scalar coupling. By applying the latter experiment to a soluble protein of about 15 kD with a similar labeling pattern an intensity decrease of about 10% was seen for an amide signal with a ^{13}C enriched adjacent carbonyl carbon (data not shown). However, no positive result was obtained for rhodopsin. A TROSY version of the HSQC experiment yielded spectra with worse signal-to-noise ratio as described previously (Klein-Seetharaman et al. 2004).

Discussion

Here, we have presented a non-invasive combined solution and solid state NMR approach which relied on enrichment of specific atoms with NMR-active isotopes and resulted in the complete assignment of tryptophan backbone and partial assignment of tryptophan side-chain NH resonances in rhodopsin. The integration of solution and solid state NMR results is summarized in Fig. 5 and Table 1. Figure 5 shows a projection of the ^{15}N dimension of a ^{1}H,^{15}N HSQC of α,ε-^{15}N-Trp labeled rhodopsin (grey line) overlaid with a solid state ^{15}N CP experiment (black line). Assignments of resonances in solid state NMR spectra are labeled in blue and the assignments in solution state NMR derived either from solvent exchange or from transfer of the solid state assignments are labeled in red and italicized. Solution state NMR spectra were obtained in DM micelles, while solid state NMR spectra were obtained in the more native DOPC lipid environment. Despite the differences in environment used, there was remarkable agreement between the chemical shifts observed in solution and in solid state. This finding is consistent with recent investigations of rhodopsin in

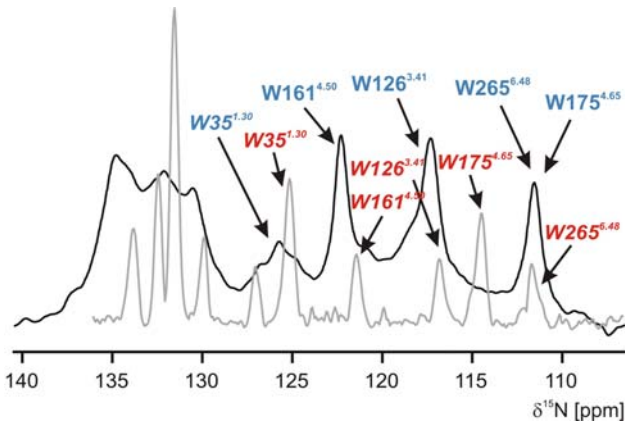

Fig. 5 Overlay of a ^{15}N detected CP experiment (black line) with an ^{15}N projection of a ^{1}H, ^{15}N HSQC spectra (grey line) of α, ε-^{15}N-Trp labeled rhodopsin. Solid state signal assignments are indicated in blue and solution state signal assignments in red. Indirectly obtained assignments are marked in italic

the dark and light-activated states by EPR spectroscopy that confirm the similarities between the results obtained in lipid bilayers and those obtained in DM (Kusnetzow et al. 2006). Further data suggest that rhodopsin displays similar thermal stability in DM and the native membrane (Ramon et al. 2003), but the Metarhodopsin II decays with a faster rate constant in DM (Arnis and Hofmann 1993). Extensive efforts to stabilize membrane proteins in micelles in a native like conformation for NMR studies have shown that empirical factors still determine which detergent is most suitable for a given protein (Page et al. 2006; Sanders and Sönnichsen 2006). Spectra of the same protein in different micellar systems often display striking differences in the chemical shift dispersion reflecting directly the suitability of the detergent. For rhodopsin, DM is the detergent that best preserves the functional and structural properties of the protein.

The overlap in chemical shifts observed in solution and in solid state allowed us to exploit the information from solution and solid state NMR complementarily. Solid state REDOR measurements resulted in the unambiguous assignment of all residues and tentative assignment of Trp35$^{1.30}$ (also labeled in italic) for which the signal to noise ratio was low. However, the ^{15}N-chemical shifts of Trp175$^{4.65}$ and Trp265$^{6.48}$ were overlapping and found both at 111.5 ppm. Solution NMR was able to compensate for these two gaps in the solid state NMR assignment. ^{1}H,^{15}N-HSQC experiments measured before and after H/D exchange in solution NMR provided evidence supporting the assignment of Trp35$^{1.30}$. Furthermore, the change in environment from DOPC to DM resulted in a strong shift of the Trp175$^{4.65}$ but not the Trp265$^{6.48}$ resonance, such that these two peaks are now well-resolved. The tentative Trp175$^{4.65}$ resonance assignment was asserted through H/D exchange. The shift in Trp175$^{4.65}$ when going from DOPC to DM is not surprising because this tryptophan is located at the membrane/water interface in contrast to Trp265$^{6.48}$, which is located in the transmembrane region facing the interior of the protein. Based on these locations, the chemical shift of the Trp175$^{4.65}$ resonance would be expected to show a dependence of detergent/lipid used, while the chemical shift of the Trp265$^{6.48}$ would be expected to be independent of the detergent/lipid environment.

Table 1 Solid state and solution NMR assignment of ^{15}N signals and solution NMR assignment of $^{1}H^{N}$ signals of α, ε-^{15}N labeled rhodopsin

Amino acid position	δ^{N}_{solid}	$\delta^{N}_{solution}$	$\delta^{H^N}_{solution}$
Trp35$^{1.30}$	125.7	125.0	7.7
Trp126$^{3.41}$	117.3	116.7	8.7
Trp161$^{4.50}$	122.3	121.3	7.2
Trp175$^{4.65}$	111.5	114.4	8.3
Trp265$^{6.48}$	111.5	111.6	8.2

The similarity in chemical shifts observed for rhodopsin studied in solution and in solid state is in agreement with comparisons between the two approaches made for other proteins. For example, very good agreements were found in the earliest comparisons for the ^{15}N chemical shifts of staphylococcal nuclease (Cole et al. 1988). Comparison of ^{13}C chemical shifts of the soluble peptides and proteins antamanide (Detken et al. 2001) and kaliotoxin (Lange et al. 2005; Lange et al. 2006), bovine pancreatic trypsin inhibitor (BPTI) (McDermott et al. 2000), the α-spectrin SH3 domain (Pauli et al. 2001; van Rossum et al. 2001, 2003; Castellani et al. 2002), the catabolite repression histidine-containing phosphocarrier protein Crh (Bockmann et al. 2003), ubiquitin (Igumenova et al. 2004a, b; Seidel et al. 2005; Zech et al. 2005), the disulfide reductase thioredoxin (Marulanda et al. 2004) and the β1 immunoglobulin binding domain of protein G (GB1) (Franks et al. 2005) show that solution and solid state values agree within 1 ppm. ^{15}N chemical shifts show somewhat larger deviations with a mean value of approx. 2 ppm because of the stronger dependence of ^{15}N chemical shifts on the electrostatic environment. Less information is available for membrane proteins. Partial assignments exist for the light-harvesting protein complex (Gammeren et al. 2005), the outer-membrane protein G (Hiller et al. 2005) and sensory rhodopsin II (Etzkorn et al. 2006) and structures have

been determined for helical peptides such as gramicidin (Arseniev et al. 1985; Ketchem et al. 1993), the 40 amino acid containing transmembrane domain of the HIV protein Vpu (Sharpe et al. 2006) and the 52 amino acid containing phospholamban (Andronesi et al. 2005). The structure of gramicidin in solution and in solid state was very similar (Arseniev et al. 1985; Ketchem et al. 1993), while Vpu and phospholamban showed somewhat larger structural differences. However, the length of the transmembrane domain of the Vpu fragment differs (Park et al. 2003; Sharpe et al. 2006) and parts of the phospholamban helix present in solution is structurally disordered in the solid state (Zamoon et al. 2003; Andronesi et al. 2005).

In several of these studies, it was the combination between solid state and solution state NMR spectroscopy, that has made possible resonance assignments, structure calculations and determinations of the orientation of the proteins in lipids (Park et al. 2003). In the case of sensory rhodopsin, a seven transmembrane protein similar in size and overall architecture to rhodopsin, rigid segments were assigned based on polarization exchange between water and the protein, while the flexible loops and the C-terminus were assigned using scalar transfer, a principle usually applied in the liquid state (Etzkorn et al. 2006). This study emphasizes in particular the utility of the combined approach to study protein dynamics. Thus, these examples, and the results presented here suggest that a complementary approach combining solution and solid state NMR may be generally applicable to other membrane proteins and may prove particularly useful for large membrane proteins like rhodopsin where full structure determinations are not possible and where the need for understanding the role of protein dynamics for protein function is critical.

References

Andronesi OC, Becker S, Seidel K, Heise H, Young HS, Baldus M (2005) Determination of membrane protein structure and dynamics by magic-angle-spinning solid-state NMR spectroscopy. J Am Chem Soc 127:12965–12974

Arnis S, Hofmann KP (1993) Two different forms of metarhodopsin II: Schiff base deprotonation precedes proton uptake and signaling state. Proc Natl Acad Sci USA 90:7849–7853

Arseniev AS, Barsukov IL, Bystrov VF, Lomize AL, Ovchinnikov Yu A (1985) 1H-NMR study of gramicidin A transmembrane ion channel. Head-to-head right-handed, single-stranded helices. FEBS Lett 186:168–174

Ballesteros J, Weinstein H (1995) Integrated methods for modeling G-protein coupled receptors. Methods Neurosci 25:366–428

Bockmann A, Lange A, Galinier A, Luca S, Giraud N, Juy M, Heise H, Montserret R, Penin F, Baldus M (2003) Solid state NMR sequential resonance assignments and conformational analysis of the 2×10.4 kDa dimeric form of the Bacillus subtilis protein Crh. J Biomol NMR 27:323–339

Carravetta M, Zhao X, Johannessen OG, Lai WC, Verhoeven MA, Bovee-Geurts PH, Verdegem PJ, Kiihne S, Luthman H, de Groot HJ, de Grip WJ, Lugtenburg J, Levitt MH (2004) Protein-induced bonding perturbation of the rhodopsin chromophore detected by double-quantum solid-state NMR. J Am Chem Soc 126:3948–3953

Castellani F, van Rossum B, Diehl A, Schubert M, Rehbein K, Oschkinat H (2002) Structure of a protein determined by solid-state magic-angle-spinning NMR spectroscopy. Nature 420:98–102

Chabre M, Breton J (1979) Orientation of aromatic residues in rhodopsin. Rotation of one tryptophan upon the meta I to meta II transition afer illumination. Photochem Photobiol 30:295–299

Cole HB, Sparks SW, Torchia DA (1988) Comparison of the solution and crystal structures of staphylococcal nuclease with 13C and 15N chemical shifts used as structural fingerprints. Proc Natl Acad Sci USA 85:6362–6365

Crocker E, Eilers M, Ahuja S, Hornak V, Hirshfeld A, Sheves M, Smith SO (2006) Location of Trp265 in metarhodopsin II: implications for the activation mechanism of the visual receptor rhodopsin. J Mol Biol 357:163–172

Detken A, Hardy EH, Ernst M, Kainosho M, Kawakami T, Aimoto S, Meier BH (2001) Methods for sequential resonance assignment in solid, uniformly 13C, 15N labelled peptides: quantification and application to antamanide. J Biomol NMR 20:203–221

Eilers M, Ying W, Reeves PJ, Khorana HG, Smith SO (2002) Magic angle spinning nuclear magnetic resonance of isotopically labeled rhodopsin. Methods Enzymol 343:212–222

Etzkorn M, Martell S, Andronesi OC, Seidel K, Engelhard M, Baldus M (2006) Secondary structure, dynamics, and topology of a seven-helix receptor in native membranes, studied by solid-state NMR spectroscopy. Angew Chem Int Ed Engl 46(3):459–462

Feng X, Verdegem PJ, Eden M, Sandstrom D, Lee YK, Bovee-Geurts PH, de Grip WJ, Lugtenburg J, de Groot HJ, Levitt MH (2000) Determination of a molecular torsional angle in the metarhodopsin-I photointermediate of rhodopsin by double-quantum solid-state NMR. J Biomol NMR 16:1–8

Franks WT, Zhou DH, Wylie BJ, Money BG, Graesser DT, Frericks HL, Sahota G, Rienstra CM (2005) Magic-angle spinning solid-state NMR spectroscopy of the beta1 immunoglobulin binding domain of protein G (GB1): 15N and 13C chemical shift assignments and conformational analysis. J Am Chem Soc 127:12291–12305

Gammeren AJ, Hulsbergen FB, Hollander JG, Groot HJ (2005) Residual backbone and side-chain 13C and 15N resonance assignments of the intrinsic transmembrane light-harvesting 2 protein complex by solid-state magic angle spinning NMR spectroscopy. J Biomol NMR 31:279–293

Getmanova E, Patel AB, Klein-Seetharaman J, Loewen MC, Reeves PJ, Friedman N, Sheves M, Smith SO, Khorana HG (2004) NMR spectroscopy of phosphorylated wild-type rhodopsin: mobility of the phosphorylated C-terminus of rhodopsin in the dark and upon light activation. Biochemistry 43:1126–1133

Gullion T, Schaefer J (1989) Rotational-echo double-resonance NMR. J Mag Res 81:196–200

Hiller M, Krabben L, Vinothkumar KR, Castellani F, van Rossum BJ, Kuhlbrandt W, Oschkinat H (2005) Solid-state magic-angle spinning NMR of outer-membrane protein G from *Escherichia coli*. Chembiochem 6:1679–1684

Hubbell WL, Altenbach C, Hubbell CM, Khorana HG (2003) Rhodopsin structure, dynamics, and activation: a perspective from crystallography, site-directed spin labeling, sulfhydryl reactivity, and disulfide cross-linking. Adv Protein Chem 63:243–290

Igumenova TI, McDermott AE, Zilm KW, Martin RW, Paulson EK, Wand AJ (2004a) Assignments of carbon NMR resonances for microcrystalline ubiquitin. J Am Chem Soc 126:6720–6727

Igumenova TI, Wand AJ, McDermott AE (2004b) Assignment of the backbone resonances for microcrystalline ubiquitin. J Am Chem Soc 126:5323–5331

Isin B, Rader AJ, Dhiman H, Klein-Seetharaman J, Bahar I (2006) Predisposition of the dark state of rhodopsin to functional changes in structure. Proteins: Structure, Function and Bioinformatics 65(4):970–983

Jastrzebska B, Maeda T, Zhu L, Fotiadis D, Filipek S, Engel A, Stenkamp RE, Palczewski K (2004) Functional characterization of rhodopsin monomers and dimers in detergents. J Biol Chem 279:54663–54675

Ketchem RR, Hu W, Cross TA (1993) High-resolution conformation of gramicidin A in a lipid bilayer by solid-state NMR. Science 261:1457–1460

Klein-Seetharaman J, Getmanova EV, Loewen MC, Reeves PJ, Khorana HG (1999) NMR spectroscopy in studies of light-induced structural changes in mammalian rhodopsin: applicability of solution (19)F NMR. Proc Natl Acad Sci USA 96:13744–13749

Klein-Seetharaman J, Reeves PJ, Loewen MC, Getmanova EV, Chung J, Schwalbe H, Wright PE, Khorana HG (2002) Solution NMR spectroscopy of [alpha –15N]lysine-labeled rhodopsin: the single peak observed in both conventional and TROSY-type HSQC spectra is ascribed to Lys-339 in the carboxyl-terminal peptide sequence. Proc Natl Acad Sci USA 99:3452–3457

Klein-Seetharaman J, Yanamala NV, Javeed F, Reeves PJ, Getmanova EV, Loewen MC, Schwalbe H, Khorana HG (2004) Differential dynamics in the G protein-coupled receptor rhodopsin revealed by solution NMR. Proc Natl Acad Sci USA 101:3409–3413

Knowles A, Priestley A (1978) The preparation of 11-cis-retinal. Vision Res 18:115–116

Kusnetzow AK, Altenbach C, Hubbell WL (2006) Conformational states and dynamics of rhodopsin in micelles and bilayers. Biochemistry 45:5538–5550

Lange A, Becker S, Seidel K, Giller K, Pongs O, Baldus M (2005) A concept for rapid protein-structure determination by solid-state NMR spectroscopy. Angew Chem Int Ed Engl 44:2089–2092

Lange A, Giller K, Hornig S, Martin-Eauclaire MF, Pongs O, Becker S, Baldus M (2006) Toxin-induced conformational changes in a potassium channel revealed by solid-state NMR. Nature 440:959–962

Li J, Edwards PC, Burghammer M, Villa C, Schertler GF (2004) Structure of bovine rhodopsin in a trigonal crystal form. J Mol Biol 343:1409–1438

Lin SW, Sakmar TP (1996) Specific tryptophan UV-absorbance changes are probes of the transition of rhodopsin to its active state. Biochemistry 35:11149–11159

Loewen MC, Klein-Seetharaman J, Getmanova EV, Reeves PJ, Schwalbe H, Khorana HG (2001) Solution 19F nuclear Overhauser effects in structural studies of the cytoplasmic domain of mammalian rhodopsin. Proc Natl Acad Sci USA 98:4888–4892

Marulanda D, Tasayco ML, McDermott A, Cataldi M, Arriaran V, Polenova T (2004) Magic angle spinning solid-state NMR spectroscopy for structural studies of protein interfaces. Resonance assignments of differentially enriched *Escherichia coli* thioredoxin reassembled by fragment complementation. J Am Chem Soc 126:16608–16620

Mason AJ, Turner GJ, Glaubitz C (2005) Conformational heterogeneity of transmembrane residues after the Schiff base reprotonation of bacteriorhodopsin: 15N CPMAS NMR of D85N/T170C membranes. FEBS J 272:2152–2164

McDermott A, Polenova T, Bockmann A, Zilm KW, Paulson EK, Martin RW, Montelione GT (2000) Partial NMR assignments for uniformly (13C, 15N)-enriched BPTI in the solid state. J Biomol NMR 16:209–219

Metz G, Wu XL, Smith SO (1994) Ramped-amplitude cross polarization in magic-angle-spinning NMR. J Mag Res Ser A 110:219–227

Nakayama TA, Khorana HG (1990) Orientation of retinal in bovine rhodopsin determined by cross-linking using a photoactivatable analog of 11-cis-retinal. J Biol Chem 265:15762–15769

Nakayama TA, Khorana HG (1991) Mapping of the amino acids in membrane-embedded helices that interact with the retinal chromophore in bovine rhodopsin. J Biol Chem 266:4269–4275

Oprian DD, Molday RS, Kaufman RJ, Khorana HG (1987) Expression of a synthetic bovine rhodopsin gene in monkey kidney cells. Proc Natl Acad Sci USA 84:8874–8878

Page RC, Moore JD, Nguyen HB, Sharma M, Chase R, Gao FP, Mobley CK, Sanders CR, Ma L, Sonnichsen FD, Lee S, Howell SC, Opella SJ, Cross TA (2006) Comprehensive evaluation of solution nuclear magnetic resonance spectroscopy sample preparation for helical integral membrane proteins. J Struct Funct Genomics 7:51–64

Palczewski K, Kumasaka T, Hori T, Behnke CA, Motoshima H, Fox BA, Le Trong I, Teller DC, Okada T, Stenkamp RE, Yamamoto M, Miyano M (2000) Crystal structure of rhodopsin: a G protein-coupled receptor. Science 289:739–745

Park SH, Mrse AA, Nevzorov AA, Mesleh MF, Oblatt-Montal M, Montal M, Opella SJ (2003) Three-dimensional structure of the channel-forming trans-membrane domain of virus protein ''u'' (Vpu) from HIV-1. J Mol Biol 333:409–424

Patel AB, Crocker E, Eilers M, Hirshfeld A, Sheves M, Smith SO (2004) Coupling of retinal isomerization to the activation of rhodopsin. Proc Natl Acad Sci USA 101:10048–10053

Patel AB, Crocker E, Reeves PJ, Getmanova EV, Eilers M, Khorana HG, Smith SO (2005) Changes in interhelical hydrogen bonding upon rhodopsin activation. J Mol Biol 347:803–812

Pauli J, Baldus M, van Rossum B, de Groot H, Oschkinat H (2001) Backbone and side-chain 13C and 15N signal assignments of the alpha-spectrin SH3 domain by magic angle spinning solid-state NMR at 17.6 Tesla. Chembiochem 2:272–281

Piotto M, Saudek V, Sklenar V (1992) Gradient-tailored excitation for single-quantum NMR spectroscopy of aqueous solutions. J Biomol NMR 2:661–665

Rafferty CN, Muellenberg CG, Shichi H (1980) Tryptophan in bovine rhodopsin: its content, spectral properties and environment. Biochemistry 19:2145–2151

Ramon E, Marrion J, del Valle L, Bosch L, Andres A, Manyos J, Garriga P (2003) Effect of dodecyl maltoside detergent on rhodopsin stability and function. Vision Res 43:3055–3061

Reeves PJ, Hwa J, Khorana HG (1999) Structure and function in rhodopsin: kinetic studies of retinal binding to purified opsin mutants in defined phospholipid-detergent mixtures serve as probes of the retinal binding pocket. Proc Natl Acad Sci USA 96:1927–1931

Reeves PJ, Kim JM, Khorana HG (2002) Structure and function in rhodopsin: a tetracycline-inducible system in stable mammalian cell lines for high-level expression of opsin mutants. Proc Natl Acad Sci USA 99:13413–13418

Reeves PJ, Thurmond RL, Khorana HG (1996) Structure and function in rhodopsin: high level expression of a synthetic bovine opsin gene and its mutants in stable mammalian cell lines. Proc Natl Acad Sci USA 93:11487–11492

Salom D, Lodowski DT, Stenkamp RE, Trong IL, Golczak M, Jastrzebska B, Harris T, Ballesteros JA, Palczewski K (2006) Crystal structure of a photoactivated deprotonated intermediate of rhodopsin. Proc Natl Acad Sci USA 103:16123–16128

Sanders CR, Sönnichsen F (2006) Solution NMR of membrane proteins: parctice and challanges. Magn Reson Chem 44:S24–S40

Seidel K, Etzkorn M, Heise H, Becker S, Baldus M (2005) High-resolution solid-state NMR studies on uniformly [13C,15N]-labeled ubiquitin. Chembiochem 6:1638–1647

Sharpe S, Yau WM, Tycko R (2006) Structure and dynamics of the HIV-1 Vpu transmembrane domain revealed by solid-state NMR with magic-angle spinning. Biochemistry 45:918–933

Spooner PJ, Sharples JM, Goodall SC, Bovee-Geurts PH, Verhoeven MA, Lugtenburg J, Pistorius AM, Degrip WJ, Watts A (2004) The ring of the rhodopsin chromophore in a hydrophobic activation switch within the binding pocket. J Mol Biol 343:719–730

van Rossum BJ, Castellani F, Pauli J, Rehbein K, Hollander J, de Groot HJ, Oschkinat H (2003) Assignment of amide proton signals by combined evaluation of HN, NN and HNCA MAS-NMR correlation spectra. J Biomol NMR 25:217–223

van Rossum BJ, Castellani F, Rehbein K, Pauli J, Oschkinat H (2001) Assignment of the nonexchanging protons of the alpha-spectrin SH3 domain by two- and three-dimensional 1H-13C solid-state magic-angle spinning NMR and comparison of solution and solid-state proton chemical shifts. Chembiochem 2:906–914

van Rossum B-J, Förster H, de Groot HJM (1997) High-field and high-speed CP-MAS13C NMR heteronuclear dipolar-correlation spectroscopy of solids with frequency-switched Lee–Goldburg homonuclear decoupling. J Mag Res 124:516–519

Verdegem PJ, Bovee-Geurts PH, de Grip WJ, Lugtenburg J, de Groot HJ (1999) Retinylidene ligand structure in bovine rhodopsin, metarhodopsin-I, and 10-methylrhodopsin from internuclear distance measurements using 13C-labeling and 1-D rotational resonance MAS NMR. Biochemistry 38:11316–11324

Zamoon J, Mascioni A, Thomas DD, Veglia G (2003) NMR solution structure and topological orientation of monomeric phospholamban in dodecylphosphocholine micelles. Biophys J 85:2589–2598

Zech SG, Wand AJ, McDermott AE (2005) Protein structure determination by high-resolution solid-state NMR spectroscopy: application to microcrystalline ubiquitin. J Am Chem Soc 127:8618–8626